Molecular Crystals and Liquid Crystals
Publication details, including instructions for authors and subscription information:
http://www.tandfonline.com/loi/gmcl20

Passive Amplification Effect in Thin Pyroelectric Films

S. V. Yablonskii [a] & E. A. Soto-Bustamante [b]

[a] Institute of Crystallography, Russian Academy of Sciences, Moscow, Russia

[b] Universidad de Chile, Facultad de Ciencias Químicas y Farmacéuticas, Santiago, Chile

Version of record first published: 30 Jun 2011

To cite this article: S. V. Yablonskii & E. A. Soto-Bustamante (2011): Passive Amplification Effect in Thin Pyroelectric Films, Molecular Crystals and Liquid Crystals, 541:1, 44/[282]-52/[290]

To link to this article: http://dx.doi.org/10.1080/15421406.2011.570122

Mol. Cryst. Liq. Cryst., Vol. 541: pp. 44/[282]–52/[290], 2011

ISSN: 1542-1406 print/1563-5287 online
DOI: 10.1080/15421406.2011.570122

Passive Amplification Effect in Thin Pyroelectric Films

S. V. YABLONSKII[1] AND E. A. SOTO-BUSTAMANTE[2]

[1]Institute of Crystallography, Russian Academy of Sciences, Moscow, Russia
[2]Universidad de Chile, Facultad de Ciencias Químicas y Farmacéuticas, Santiago, Chile

Here we continue the description of the previously found passive amplification effect in thin pyroelectric films placed on a massive heat-conducting substrate. We show that in the definite modulation frequency range the amplification effect occurs i.e., a current generated by a thin pyroelectric film placed on substrate exceeds that in freely suspended film. The frequency dependence a pyroelectric current is illustrated by set of examples including achiral ferroelectric liquid crystals, ferroelectric polymers and polycrystalline compounds.

Keywords Ferroelectric polymers; liquid crystals; polycrystalline pyroelectrics; pyroelectric effect

1. Introduction

The pyroelectric effect is an example of a thermoelectric phenomenon which involves the generation of a current or voltage at a change of temperature [1,2]. In pyroelectric detectors, as a rule, energy of quanta of detected radiation is insufficient for excitation of an electronic subsystem of a crystal and radiant energy is used to increase the oscillatory energy of system of atoms through temperature and spontaneous polarization changes [3]. The factor of conversion of thermal energy to electricity for pyroelectric detector without a bias field is quite small, about of 1% [4]. The fundamental reason of so low conversion is due to that the necessary energy for heating of a crystal lattice considerably surpasses the energy which is required to destroy the spontaneous polarization. The large internal resistance of the pyroelectric detector also interferes with the effective transfer of electric energy from the detector to the loading resistor (the pyroelectric detector is the current generator [5]). One of the defining parameters of detectors of radiation is current sensitivity. For pyroelectric detectors it is of 1 μA/W [6], much lower than the current sensitivity of photon detectors, 1 A/W and more [7].

At the same time pyroelectric detectors possess a number of essential advantages which allow them to compete with photon detectors successfully. The important

Address correspondence to S. V. Yablonskii, Institute of Crystallography, Russian Academy of Sciences, Leninsky prosp. 59, Moscow 119333, Russia. E-mail: yablonskii2005@yandex.ru

advantage is the fact that pyroelectric detectors are not wavelength selective. For them spectral sensitivity based on units of falling power depends only on one parameter: emissivity of the pickup surface. In practice this can be close to emissivity of absolutely black body, i.e., it is equal 1 in a wide spectral interval from visible to far infra-red range. Thus, pyroelectric detectors, without demanding special cooling, are capable of detecting optical signals in spectral range inaccessible to modern photon detectors. It is necessary to note also the high-speed characteristics of a pyroelectric detector, allowing them to detect fast processes by duration of hundreds picoseconds [8]. Structurally, a pyroelectric sensor represents the capacity filled with a pyroelectric substance. As a rule, the capacity is placed on a substrate which serves as a heat-conducting path. Substrate presence essentially influences low-frequency characteristics of the detector. It is considered that maximum current sensitivity is realized for freely suspended pyroelectric films when there is no channel of loss of heat. Thus the substrate should be as thin as it is possible [9].

In the given work we will show that for a pyroelectric film located on a massive heat-conducting substrate there is a frequency interval of modulation of falling radiation where the current sensitivity behaves "abnormal". In this frequency interval there is a passive amplification of pyroelectric current in comparison to a freely suspended film. The explanation of the given effect is discussed in the results. The effect of passive amplification is illustrated by experimental examples.

2. Results of the Heat Conduction Theory of Pyroelectric Effect

A given work examines the so-called longitudinal pyroelectric effect when the direction of a Poynting vector coincides with a direction of a vector of spontaneous polarization. The basic one-dimensional configuration used throughout our experiment is represented schematically in Figure 1(a). A pyroelectric sensor is situated on massive substrate. The medium in front of the pyroelectric material is air. Falling radiation is absorbed in an electrode which sometimes becomes covered by special coverings, for example, a black alloy of silver, copper, lead and sulphur. In the case of a neglecting of volume absorption of radiant energy it is necessary to search for the temperature field $T(x, t)$, solving the equation of heat conductivity with corresponding boundary conditions. Following [9] the temperature field $T(x, t)$ for the sinusoidally amplitude-modulated radiation with circular frequency ω it is possible to present in the form:

$$T(x,t) = T_o(x) + e^{i\omega t}\Delta T(x) \qquad (1),$$

where the first term of the left part of the expression (1) defines a working point of pyroelectric detector, and the second – characterizes a variable component of a temperature increment, directly influencing signal formation in a sensitive element. The configuration of Figure 1 can be modeled theoretically by considering the case of a one-dimensional pyroelectric detector with periodic excitation. Solving the heat conducting problem for a pyroelectric of thickness h placed on substrate of thickness H we get [1,9]:

$$\frac{d^2\Delta T(x)}{dx^2} = \frac{\Delta T(x)}{L_h^2}, \quad L_h = \left(\frac{\delta_h}{i\omega c_h \rho_h}\right)^{1/2}, \quad 0 < x < h, \qquad (2)$$

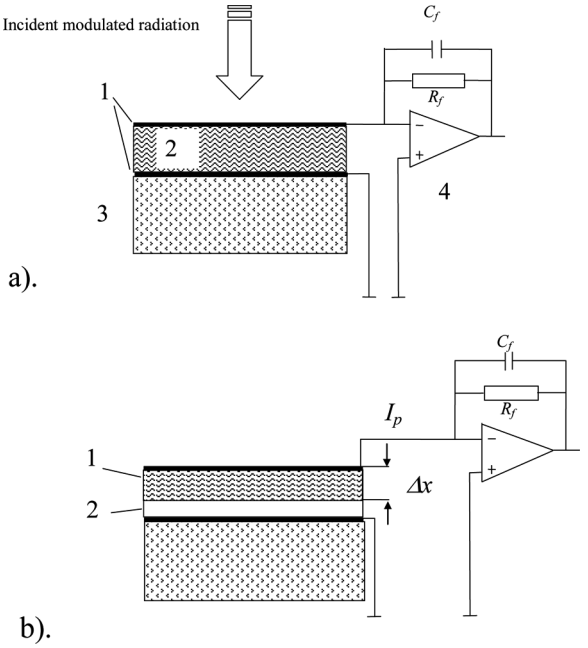

Figure 1. (a) One-dimensional geometry of the pyroelectric chip with measuring circuit: 1 – Aluminium electrodes, 2 – Pyroelectric material, 3 – Glass substrate, 4 – Lock-in-amplifier (current mode). Detector has capacitance C_p and loss resistance R_p, feedback resistor R_f, and capacitance C_f. (b) Partially filled with pyroelectric material the pyroelectric detector. 1 – Pyroelectric material, 2 – Non-polar dielectric.

$$\frac{d^2\Delta T(x)}{dx^2} = \frac{\Delta T(x)}{L_H^2}, \quad L_H = \left(\frac{\delta_H}{i\omega c_H \rho_H}\right)^{1/2}, \quad h < x < h + H, \tag{3}$$

$$\Delta T(x) = \frac{\Delta T(h)\sinh(x/L_h) + \Delta T(0)\sinh[(h-x)/L_h]}{\sinh(h/L_h)}, \quad 0 < x < h \tag{4}$$

$$\Delta T(x) = \frac{\Delta T(H)\sinh[(x-h)/L_H] + \Delta T(h)\sinh[(H+h-x)/L_H]}{\sinh(H/L_H)}, \quad h < x < h + H \tag{5}$$

The coefficients $\Delta T(0)$, $\Delta T(h)$ и $\Delta T(H)$ are detected from balances of heat flux on borders $x = 0$, h, $h + H$. Here it is neglected a heat flux from outside substrates at $x = h + H$ that is justified by using of the thick substrates. The electrodes were thin enough not to break a temperature field in the sample. The proper boundary conditions are:

$$-\delta_h \frac{d\Delta T(x)}{dx}\bigg|_{x=0+0} = \eta P_1 - g_o \Delta T(0), \tag{6}$$

$$-\delta_h \frac{d\Delta T(x)}{dx}\bigg|_{x=h-0} = -\delta_H \frac{d\Delta T(x)}{dx}\bigg|_{x=h+0}, \tag{7}$$

$$-\delta_H \frac{d\Delta T(x)}{dx}\bigg|_{x=h+H-0} = 0, \tag{8}$$

Using boundary conditions (6–8) we can get expressions for coefficients $\Delta T(0)$ and $\Delta T(h)$ in the form:

$$\Delta T(0) = \eta P_1 \left[1 + \frac{\delta_H/L_H}{\delta_h/L_h}\tanh\left(\frac{h}{L_h}\right)\tanh\left(\frac{H}{L_H}\right)\right] \times \left\{g_o\left[1 + \frac{\delta_H/L_H}{\delta_h/L_h}\tanh\left(\frac{h}{L_h}\right)\tanh\left(\frac{H}{L_H}\right) + \frac{h}{L_h}\tanh\left(\frac{h}{L_h}\right) + \frac{H}{L_H}\tanh\left(\frac{H}{L_H}\right)\right]\right\}^{-1}, \tag{9}$$

and

$$\Delta T(h) = \frac{\eta P_1}{\cosh(h/L_h)} \times \left\{g_o\left[1 + \frac{\delta_H/L_H}{\delta_h/L_h}\tanh\left(\frac{h}{L_h}\right)\tanh\left(\frac{H}{L_H}\right) + \frac{h}{L_h}\tanh\left(\frac{h}{L_h}\right) + \frac{H}{L_H}\tanh\left(\frac{H}{L_H}\right)\right]\right\}^{-1}, \tag{10}$$

The pyroelectric layer possesses heat conductivity δ_h, a specific mass thermal capacity c_h, and density ρ_h, while corresponding parameters of a substrate are designated as δ_H, c_H and ρ_H, accordingly. L_h and L_H designate lengths of temperature wave in a film and in a substrate, $i = \sqrt{-1}$, A – heated area of the sample, $P_1 \cdot e^{i\omega t}$ – incident radiation per unit area, η – absorbance of the electrode, g_o – heat transfer coefficient between the film and the surroundings.

Pyroelectric current of the detector in the case of homogeneous distribution of pyroelectric coefficient of sample γ can be extracted from the solution of an electrostatic problem as follows [1,9]:

$$I_p = \frac{iA\omega\gamma}{h} e^{i\omega t} \int_0^h \Delta T(x)dx, \tag{11}$$

In expanded form we get:

$$I_p = \frac{iA\omega\gamma\eta P_1 L_h}{h}\left[\tanh\left(\frac{h}{L_h}\right) + \frac{\delta_H/L_H}{\delta_h/L_h}\tanh\left(\frac{H}{L_H}\right)\frac{\cosh(h/L_h) - 1}{\cosh(h/L_h)}\right] \times \left\{g_o\left[1 + \frac{\delta_H/L_H}{\delta_h/L_h}\tanh\left(\frac{h}{L_h}\right)\tanh\left(\frac{H}{L_H}\right) + \frac{h}{L_h}\tanh\left(\frac{h}{L_h}\right) + \frac{H}{L_H}\tanh\left(\frac{H}{L_H}\right)\right]\right\}^{-1}. \tag{12}$$

As soon as the temperature wave expanding through a pyroelectric layer is attenuated, the generated current is described by the complex function, allowing

calculating a phase of delay of a current related to sinusoidal external modulation, and also the amplitude of a current depending on the modulation frequency. The complicated functions $T(x, t)$ and I_p, depending more than ten parameters, require a graphical analysis for expedience.

3. Results of Computational Experiment

Figures 2 (a, b) demonstrates the modulus of integral $<\Delta T>=\frac{1}{h}\int_0^x \Delta T(x)dx$ as a function of Δx, where Δx is distance from front-face surface to some point in the interior of the specimen. The functions for two different frequencies $\omega_1 = 640\,\mathrm{s}^{-1}$ and $\omega_2 = 6400\,\mathrm{s}^{-1}$ show monotonic behaviors with positive derivatives. These results are very important as confirmation of the fact that the maximum of pyroelectric current of the expression (11) can be obtained if the capacity, shown in Figure 1(b), is completely filled with a pyroelectric material. The passive amplification effect is

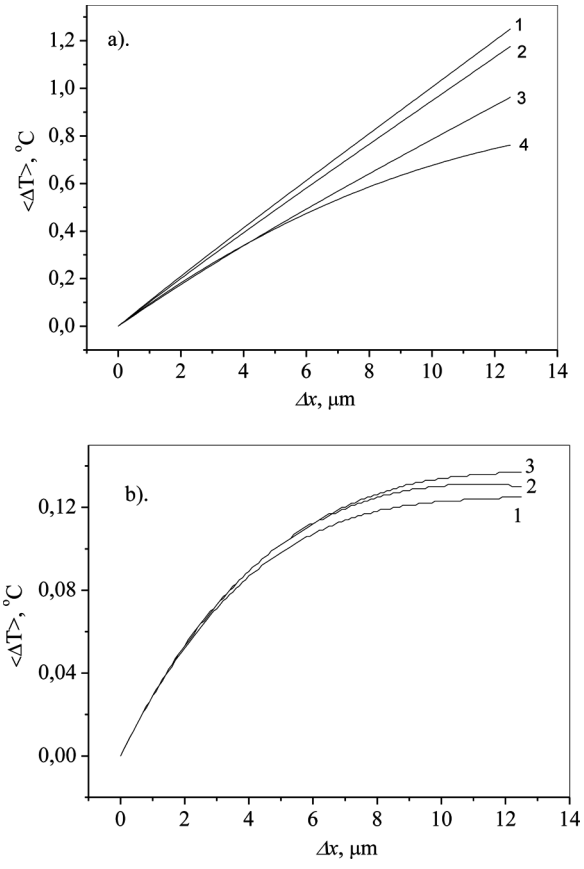

Figure 2. Graphs of the modulus of increment temperature $<\Delta T>$ averaged over a thickness of a layer as function of Δx for different substrate thicknesses H. (Δx – distance from front-face surface to some point in the interior of the specimen) ($\delta_h = 2\cdot 10^{-1}\,\mathrm{W/m\cdot K}$, $\rho_h = 10^3\,\mathrm{kg/m^3}$, $c_h = 1.95\,\mathrm{kJ/kg\cdot K}$, $\delta_H = 1\,\mathrm{W/m\cdot K}$, $\rho_H = 2.4\cdot 10^3\,\mathrm{kg/m^3}$, $c_H = 0.67\,\mathrm{kJ/kg\cdot K}$, $g_o = 6.2\,\mathrm{W/m^2\cdot K}$, $P_I = 3\cdot 10^4\,\mathrm{Вт/м^2}$, $h = 12.5\,\mu\mathrm{m}$). (a) $\omega = 640\,\mathrm{s}^{-1}$. 1 – $H = 0$, 2 – $H = 1\,\mu\mathrm{m}$, 3 – $H = 5\,\mu\mathrm{m}$, 4 – $H = 0.5\,\mathrm{cm}$. (b) $\omega = 6400\,\mathrm{s}^{-1}$. 1 – $H = 0\,\mu\mathrm{m}$, 2 – $H = 5\,\mu\mathrm{m}$, 3 – $H = 0.5\,\mathrm{cm}$.

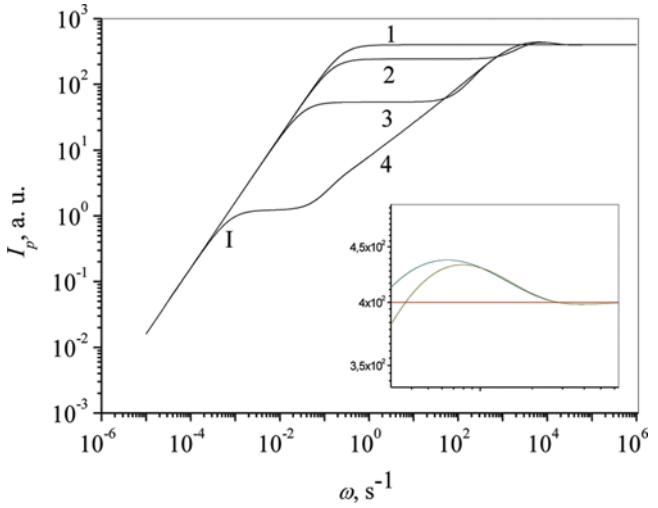

Figure 3. Plots of the pyroelectric current I_p as the function of the circular frequency ω. 1 – $H = 0\,\mu m$, 2 – $H = 10\,\mu m$, 3 – $H = 100\,\mu m$, 4 – $H = 0.5\,cm$. Insert shows the oscillatory behavior of the pyroelectric current. (Figure appears in color online.)

demonstrated in Figure 3 as modulus of pyroelectric current I_p vs. circular frequency ω. One can see the passive amplification effect at evaluated frequencies when the length of the temperature wave L_h is much less than the thickness of pyroelectric layer h. The pyroelectric current I_p demonstrates oscillatory behavior as shown in the insert to Figure 3. Figure 4 shows the deviation of maxima and minima of the pyroelectric current from that in freely suspended film as a function of substrate thicknesses.

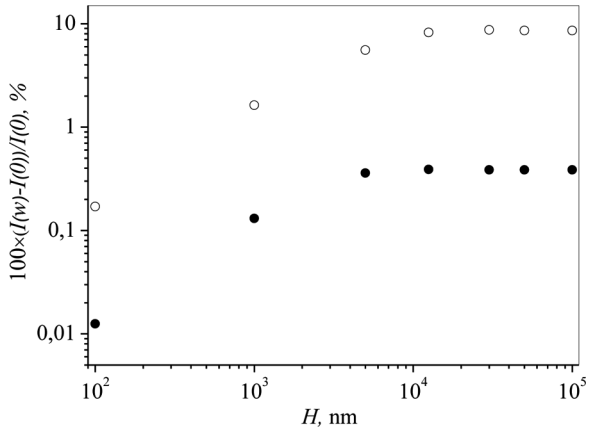

Figure 4. Excess of the first maximum pyroelectric current over its value for freely suspended film (open circles) and belittling of pyroelectric current for the first minimum (closed circles) as function of support thickness H. (Practically plots show hardly appreciable non-monotonic behavior).

4. Experimental Confirmation of Passive Amplification Effect

The methods of the preparation of the pyroelectric cells based on pyroelectric materials: tetraaminobiphenyl, mixtures of achiral liquid crystal ferroelectric polymers and their monomers (Pm6R8 + 33%m6R8) and ferroelectric copolymer (P(VDF-TrFE) 70:30% have been described elsewhere [1,2,10,11]. Thick aluminum layers evaporated onto the pyroelectric material were used as front electrodes. It ensured the equal absorbance of the evaporated electrodes. The pyroelectric current was excited by modulated radiation of the light emitting diode with wavelength of $\lambda = 675$ nm and power of $P_o = 23$ Mw. The diode radiation was modulated by rectangular impulses in a range of frequencies from 1 Hz to 250 kHz. The diameter of a beam of light falling on a film was $D = 1$ mm. It corresponds to power density of radiation of $P_I = 3 \cdot 10^4\,\mathrm{W/m^2}$. The pyroelectric current was detected by a lock-in amplifier EG&G 7260. The linearity of the frequency characteristic in a current mode of the given model of the lock-in amplifier remained up to 10 kHz (0.3 dB at 50 kHz). All measurements were made at room temperature.

The results of the experiment are shown in Figure 5. A thick film of a copolymer, $h_{cop} = 12.5$ μm, shows strongly pronounced passive amplification in the region of the linearity of the frequency characteristic of the lock-in amplifier (curve 3). For two other films (curves 1 and 2) with thicknesses, $h_{TAD} = 1.5$ μm and $h_{LC} = 0.6$ μm, oscillating behavior lies far outside of linearity of the frequency characteristic of the lock-in amplifier. In Figure 5 curves 1 and 2 only partially correspond to the true behavior of the pyroelectric current as function of frequency. In fact, above 30 kHz the nonlinear effects of the lock-in-amplifier mask the bumps corresponding to the passive amplification. In Figure 5 the frequency mode $\sqrt{\omega}$ is obtained allowing calculating the pyroelectric coefficients. Since the pyroelectric coefficient for TAD is known, $\gamma_{\mathrm{TAD}} = 50\,\mu\mathrm{C/m^2K}$ [11], it is possible to calculate the pyroelectric coefficients

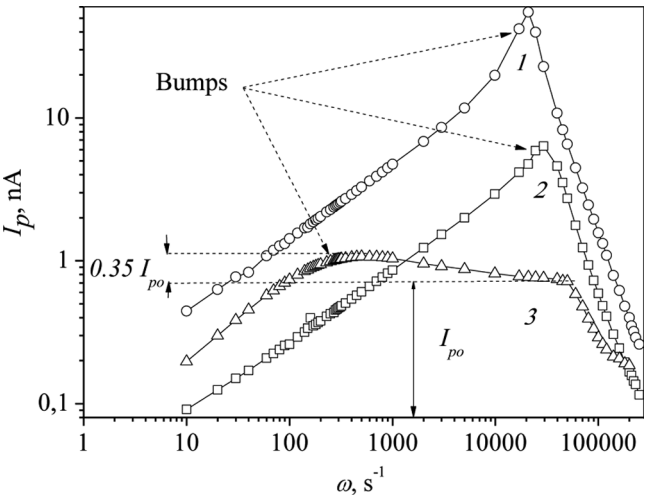

Figure 5. Experimental curves of the pyroelectric current I_p as function of circular frequency ω. *1* – Polycrystalline organic compound TAD (Tetraaminobiphenyl) [13,14], $h_{TAD} = 1.5$ μm; *2* – Glassy liquid crystalline achiral antiferroelectric mixture of polymer with its monomer [1,2], $h_{LC} = 0.6$ μm; *3* – Ferroelectric copolymer P(VDF-TrFE) 70:30%, $h_{cop} = 12.5$ μm [1,2,14].

of the copolymer and liquid crystal composition to be $\gamma_{cop} = 23.3\,\mu C/m^2K$ and $\gamma_{LC} = 10\,\mu C/m^2K$ respectively.

5. Discussion

The excess of the pyroelectric current of a copolymer film shown in Figure 5 (curve 3) over a plateau is of 0.35 I_{po} surpassed a possible theoretical maximum of 0.15 I_{po} more than twice. (The coefficient 0.15 was found by simulation according to the equation 12 by variation of the proper parameters). Such strong divergence which occurs outside the limits of experimental accuracy can be explained by the additional contribution to the pyroelectric signal. One of the possible mechanisms is the contribution from a so-called tertiary pyroelectric effect [12,13]. This effect appears in non-uniformly heated films when the gradient temperature ∇T changes symmetry and induces a polar state. In this case the tertiary pyroelectric effect is manifested as an amplification (or even attenuation) of the primary and secondary pyroelectric effects. Therefore we show that in this frequency interval the temperature distribution in the sample is strongly non-uniform.

The numerical analysis of the equation (12) unambiguously establishes that the passive amplification effect strongly correlates with the existence of the heat flux across the boundary of the pyroelectric-substrate. When thermal conductivity of substrate tends to zero, the bump corresponding amplification effect becomes insignificant. If one takes into account the thermal conductivity of air near the rear part of the supports the passive amplification bump occurs even in the low frequency range at turn-on frequency (in the position I, shown in Fig. 3) [14]. The turn-on frequency $\omega = \frac{g_o}{c_h\rho_h h + c_H\rho_H H}$ is the frequency expected from the lumped model in which the pyroelectric layer plus substrate is heated uniformly [9].

It should also be noted that the passive amplification effect was experimentally observed in [14–16], though explanations of the given effect have not been presented in the known literature to date.

6. Conclusions

The results of the given work are general and applicable to any pyroelectric material. The oscillating behavior of a pyroelecric current as the function of frequency is not explained by an interference of temperature waves [1]. It is simply a general property of the solution of heat conductivity equation with corresponding boundary conditions. Then heat conductivity of substrate tends to zero and the oscillating behavior of the pyroelectric current tends to that for freely suspended film. Besides an obvious advantage from the point of view of the improvement of stress-strain properties of a pyroelectric detector, the thick substrate can also change the current responsivity in within certain frequency ranges. Usually the effect of attenuation dominates, especially in the low-frequency range. But in the definite high-frequency range permanently passive amplification effect occurs. The amplification effect can be useful for detecting shot pulse signals.

Acknowledgment

S. V. Yablonskii thanks RFBR № 09-08-00362-a and E. A. Soto-Bustamante Fondecyt project № 1071059 for financial support.

References

[1] Yablonskii, S. V., & Soto-Bustamante, E. A. (2010). *JEPT*, *111*(5), to be published.
[2] Yablonskii, S., Soto-Bustamante, E. A., Trujillo-Rojo, V. H., & Sorokin, V. V. (2008). *J. Appl. Phys.*, *104*, 11402.
[3] Chol, G., Marfaing, Y., Munsch, M., Thorel, P., & Combette, P. (1968). *Les Détecteurs de Rayonnement Infra-Rouge*; Dunod: Paris.
[4] Fatuzzo, E., Kiess, H., & Nitsche, R. (1966). *J. Appl. Phys.*, *37*, 510.
[5] van der Ziel, A. (1974). *J. Appl. Phys.*, *45*, 4128.
[6] Yablonskii, S. V., Grossmann, S., Weyrauch, T., Werner, R., Soto-Bustamante, E. A., Haase, W., Yudin, S. G., & Blinov, L. M. (2000). *Ferroelectrics*, *247*, 343.
[7] Culp, J., Nabet, B., Castro, F., & Anwar, A. (1998). *Appl. Phys. Lett.*, *73*, 1562.
[8] Lang, S. B. (2005). *Phys. Today*, *58*, August 31.
[9] van der Ziel, A. (1973). *J. Appl. Phys.*, *44*, 546.
[10] Murtazin, A., Olihov, I., & Sokolov, D. (2006). *Elektronika: Nauka, Tehnologiya, Biznes.* (Russian), *1*, 26.
[11] Pevcov, E. F., Sigov, A. S., Maleto, M. I., & Svotina, A. P. Proceedings of 14 International symposium ≪Thin films in optics, and electronics≫. (Russian), ISTFE-14, Kharkov, p. 166, (2002).
[12] Kosorotov, V. F., Kremenchugskij, L. S., Levash, L. V., & Shchedrina, L. V. (1996). *Ferroelectrics*, *70*, 27.
[13] Kosorotov, V. F., Levash, L. V., Shedrina, L. V., Zagoruiko, Yu. A., Komar, V. K., & Fedorenko, O. A. (1994). *Kvantovaya Elektronika* (Russian), *21*, 588.
[14] Chirtoc, M., Bentefour, E. H., Antoniow, J. S., Glorieux, C., Thoen, J., Delenclos, S., Sahraoui, A. H., Longuemart, S., Kolinsky, C., & Buisine, J. M. (2003). *Rev. of Sc. Instr.*, *74*, 648.
[15] Lehman, J. H., Radojevic, A. M., Osgood, R. M., Levy, M., & Pannell, C. N. (2000). *Optics Letters*, *25*, 1657.
[16] Jyh-Jier, Ho, Fang, Y. K., Lee, W. J., Chen, F. Y., Hsieh, W. T., Ting, S. F., Ju, M. S., Huang, S. B., Wu, K. H., & Chen, C. Y. (1999). *IEEE Transaction on Electronic Devices*, *46*, 2289.